The Journal of Chemical Physics

Accounting for the exact degeneracy and quasidegeneracy in the automerization of cyclobutadiene via multireference coupled-cluster methods

Cite as: J. Chem. Phys. **131**, 114103 (2009); https://doi.org/10.1063/1.3225203
Submitted: 23 July 2009 . Accepted: 20 August 2009 . Published Online: 15 September 2009

Xiangzhu Li, and Josef Paldus

View Online Export Citation

ARTICLES YOU MAY BE INTERESTED IN

Automerization reaction of cyclobutadiene and its barrier height: An ab initio benchmark multireference average-quadratic coupled cluster study
The Journal of Chemical Physics **125**, 064310 (2006); https://doi.org/10.1063/1.2222366

Perspective: Multireference coupled cluster theories of dynamical electron correlation
The Journal of Chemical Physics **149**, 030901 (2018); https://doi.org/10.1063/1.5039496

Iterative perturbation calculations of ground and excited state energies from multiconfigurational zeroth-order wavefunctions
The Journal of Chemical Physics **58**, 5745 (1973); https://doi.org/10.1063/1.1679199

AIP Publishing

© 2009 American Institute of Physics.

Accounting for the exact degeneracy and quasidegeneracy in the automerization of cyclobutadiene via multireference coupled-cluster methods

Xiangzhu Li[a] and Josef Paldus[b]
Department of Applied Mathematics, University of Waterloo, Waterloo, Ontario N2L 3G1, Canada

(Received 23 July 2009; accepted 20 August 2009; published online 15 September 2009)

The automerization of cyclobutadiene (CBD) is employed to test the performance of the reduced multireference (RMR) coupled-cluster (CC) method with singles and doubles (RMR CCSD) that employs a modest-size MR CISD wave function as an external source for the most important (primary) triples and quadruples in order to account for the nondynamic correlation effects in the presence of quasidegeneracy, as well as of its perturbatively corrected version accounting for the remaining (secondary) triples [RMR CCSD(T)]. The experimental results are compared with those obtained by the standard CCSD and CCSD(T) methods, by the state universal (SU) MR CCSD and its state selective or state specific (SS) version as formulated by Mukherjee *et al.* (SS MRCC or MkMRCC) and, wherever available, by the Brillouin–Wigner MRCC [MR BWCCSD(T)] method. Both restricted Hartree-Fock (RHF) and multiconfigurational self-consistent field (MCSCF) molecular orbitals are employed. For a smaller STO-3G basis set we also make a comparison with the exact full configuration interaction (FCI) results. Both fundamental vibrational energies—as obtained via the integral averaging method (IAM) that can handle anomalous potentials and automatically accounts for anharmonicity– and the CBD automerization barrier for the interconversion of the two rectangular structures are considered. It is shown that the RMR CCSD(T) potential has the smallest nonparallelism error relative to the FCI potential and the corresponding fundamental vibrational frequencies compare reasonably well with the experimental ones and are very close to those recently obtained by other authors. The effect of anharmonicity is assessed using the second-order perturbation theory (MP2). Finally, the invariance of the RMR CC methods with respect to orbital rotations is also examined. © *2009 American Institute of Physics*.
[doi:10.1063/1.3225203]

I. INTRODUCTION

For closed-shell type, lowest-lying states of a given symmetry species, the single-reference (SR) coupled-cluster (CC) methods[1–3] accounting for one- and two-body cluster amplitudes, as represented by the standard CC method with singles and doubles[4] (CCSD), particularly when perturbatively corrected for triples [CCSD(T) method[5]], represent an excellent post-Hartree–Fock approaches to the many-electron correlation problem assuming that the state considered is nondegenerate (for reviews, see, e.g., Refs. 6–11; for a historical overview, see Refs. 12 and 13). It is well known, however, that with the increasing quasidegeneracy of the reference configuration $|\Phi_0\rangle$ the importance of higher-than-pair clusters [i.e., triples (T), quadruples (Q), etc.] also increases and, consequently, the accuracy of the CCSD approximation deteriorates. For a sufficiently strong quasidegeneracy, even the perturbative (T)-correction for triples becomes problematic, resulting in a gross overestimate of computed energies or even in a complete breakdown, thus invalidating the usefulness of the CCSD(T) approach. This situation invariably arises when considering dissociation channels involving genuine chemical bonds and leading to open-shell fragments or, generally, when considering open-shell states possessing a multireference (MR) character, as encountered in various radicals or biradicals (see, e.g., Refs. 6, 8, 9, 11, and 14–16). Clearly, such cases require MR-type approaches that are based on a sufficiently large model or reference space that is capable to provide an adequate, size-consistent, zero-order description.

The genuine MR CC approaches of either the valence universal (VU)[17–19] or the state universal[20] (SU) kind describe exact degeneracy very well, but, unfortunately, are often faced with a number of practical problems (intruder states, the requirement of a model space completeness, complexity of the resulting algorithms, and the implied computational demands; see, e.g., Refs. 8, 9, 11, 21, and 22). Thus, most of the recently exploited MR approaches are of the state-specific or state-selective (SS) type, focusing on one state at a time (for an excellent overview, see Ref. 23). These approaches rely on either the MR SU CCSD approach,[20] leading to the SS MRCC or (Mukherjee) MkCCSD method,[24–31] or on the Brillouin–Wigner (BW) CCSD MRCC method.[32–39]

In addition to these "genuine" SS versions of the MR SU

[a]Electronic mail: xli@scienide.uwaterloo.ca.
[b]Also at Department of Chemistry and GWC[2], Waterloo Campus, University of Waterloo, Waterloo, Ontario N2L 3G1, Canada.

 © 2009 American Institute of Physics

CC method, one also employs essentially SR-type approaches that correct for the effect of higher-than-pair clusters either via the "internal" or via the "external" corrections. The internally corrected approaches rely either on the many-body perturbation theory (MBPT), as does the above mentioned CCSD(T) method, or on some approximate version of higher-order SR CC equations [e.g., the completely renormalized CR-CC(2,n) methods[40–45] or partially linearized MR CCSD methods[46,47]] and, consequently, are fully size extensive. In contrast, the externally corrected ecCCSD methods[48–55] employ some external (i.e., non-CC or MBPT) wave function as a source of higher-than-pair clusters, such as a variational MR CISD (configuration interaction with singles and doubles) wave function in the case of the RMR CCSD methods.[56–60] The external source wave function must be capable to properly describe the desired dissociation channel or the considered radical species, being based on an appropriate size-consistent, zero-order reference space, and must be able to supply a small, but representative, subset of the most important (primary) triples and quadruples. The remaining (secondary) triples are then sufficiently small to allow a perturbative treatment as in the standard SR CCSD(T) method, leading to the RMR CCSD(T) approach.[61] Moreover, when the model space is complete, the RMR CCSD energy is invariant with respect to occupied-occupied and virtual-virtual orbital rotations. Finally, it may slightly violate the exact size extensivity in spite of the exponential ansatz for the wave function.

The RMR CCSD-type methods proved to be very successful in generating adiabatic potentials in the entire range of geometries including those with highly stretched bonds,[60] even when dissociating a triple bond.[14] They also provide superior results when handling radical species, from the small yet challenging BN, C_2, BNB, and N_3 molecules[15,16,62,63] to medium-sized organic diradicals such as benzyne,[64] pyridyne,[65] or naphthyne.[66] In this paper we apply these methods to the automerization of cyclobutadiene (CBD). This prototypical antiaromatic, π-electron, highly strained, and thus highly reactive and short-lived system represents a challenge for both theory and experiment[67–81] (for additional references, see Ref. 78). It thus represents an excellent probing ground for testing the efficiency of various approaches in their ability to account for quasidegeneracy ranging from the full degeneracy in its square configuration to nondegenerate, or only very weakly quasidegenerate, rectangular conformations, not unlike the four-hydrogen system (P4 model) considered earlier.[82]

The objectives of this study is, therefore, to assess the performance of the RMR CCSD and RMR CCSD(T) methods in their ability to describe the potential energy curves (PECs) or surfaces (PESs) and the implied barrier height and vibrational frequencies for this system by comparing it with the performance of other MR CC approaches, in particular those of the SU, SS (or Mk), and BW type. This is accomplished by comparing these results with experiment, assessing at the same time the reliability of the recently introduced integral averaging method (IAM) for the computation of fundamental vibrational frequencies.[83]

The principal methods employed are briefly described in the next section (Sec. II). Since the above mentioned invariance of the RMR CCSD method to orbital rotations has not yet been numerically tested, we illustrate the degree of this invariance in Sec. III for the case of CBD. Other computational aspects are presented in Sec. IV. The results and their discussion are the subject of Sec. V and the conclusions are drawn in Sec. VI.

II. METHODS

We now briefly comment on those CC methods that are employed in this work. Genuine MR SU CC approaches, be they of the general[20] or SS kind, are most appropriate when dealing with exactly or almost exactly degenerate states, while their performance deteriorates when the state of interest acquires a SR character. In contrast, the RMR-type approaches have inherently a one state character, so that they naturally reduce to the standard SR CCSD or SR CCSD(T) methods in the absence of degeneracy. They employ a SR CC *ansatz* that is based on a leading independent particle model configuration and account for its quasidegeneracy via the external, primary triples and quadruples, as provided by an MR CISD wave function [and, in the case of RMR CCSD(T), also via the standard (T)-correction for the secondary triples] within the standard SR CCSD formalism.[56] Consequently, since they do not treat all the quasidegenerate configurations on an equal footing, they are unable to recover the exact degeneracy (unless, of course, the triples and quadruples would stem from the exact FCI wave function, the fact of only a theoretical interest). The RMR-type methods[56,61] and their implementation and performance have been adequately documented in the literature.[14,57–60,62–66,84–94] We thus focus on closely related genuine SU and SS CC methods. Relying on this relationship we implemented the SS (or Mk) CCSD method in our CC package by relying on our general-model-space (GMS) SU CCSD codes.

Both the full SU and SS MR CC methods employ the Jeziorski and Monkhorst *ansatz* for the wave operator.[20] The wave function for the αth state $|\Psi_\alpha\rangle$ has the form

$$|\Psi_\alpha\rangle = \sum_{i=1}^{M} c_{i\alpha} e^{T(i)} |\Phi_i\rangle, \tag{1}$$

where $T(i)$ designates the cluster operator that is associated with the reference $|\Phi_i\rangle$ and is expressed as a linear combinations of excitation operators $G_j^{(k)}(i)$ of excitation level k, i.e.,

$$T(i) = \sum_k T_k(i) = \sum_{j,k} t_j^{(k)}(i) G_j^{(k)}(i), \tag{2}$$

with $t_j^{(k)}$ designating the corresponding cluster amplitudes. Here the subscript j enumerates distinct excitation operators and implicitly defines k [so that we can drop the superscript (k) once we know the explicit form of j]. In the MR CCSD case we have that $k=1,2$.

The $c_{i\alpha}$ coefficients, Eq. (1), are given by the components of the eigenvectors of the effective Hamiltonian (cf., e.g., Refs. 8, 9, 21, and 22). The cluster amplitudes are then obtained by solving the appropriate MR CC equations that are different for the standard SU and SS methods. We shall

TABLE I. The numerical test of the noninvariance of the RMR CCSD and RMR CCSD(T) methods with respect to orbital rotations, as compared with CCSD and CCSD(T), for the rectangular cyclobutadiene conformer using a DH basis set (Ref. 100). The rotation always mixes two orbitals of a different kind by 15°. The RMR methods employ two references and only the valence electrons are correlated unless indicated otherwise. The effect of orbital rotation is measured by the energy differences (in a.u.) between the results obtained with rotated and unrotated orbitals.

Orbitals (type, symmetry)	CCSD	CCSD(T)	RMR CCSD	RMR CCSD(T)
1,5 (occupied-occupied, a_g,a_g)[a]	$<10^{-6}$	0.000 100	$<10^{-6}$	0.000 090
9,11 (occupied-occupied, a_g,a_g)	$<10^{-6}$	0.000 006	$<10^{-6}$	0.000 005
11,12 (occupied-occupied, a_g,b_{3u})	$<10^{-6}$	0.000 001	$<10^{-6}$	0.000 001
16,21 (virtual-virtual, b_{1u},b_{1u})	$<10^{-6}$	0.000 002	$<10^{-6}$	0.000 001
16,18 (virtual-virtual, b_{1u},b_{2u})	$<10^{-6}$	$<10^{-6}$	$<10^{-6}$	$<10^{-6}$
14,15 (active-active, b_{1g},b_{2g})	−0.000 243	−0.000 435	0.000 493	0.000 117
14,15 (active-active, b_{1g},b_{2g})[b]			−0.000 015	−0.000 525
14,15 (active-active, b_{1g},b_{2g})[c]			−0.000 022	−0.000 618

[a]The results given in this row were obtained by correlating all the electrons.
[b]The RMR results given in this row used four references, since the rotated MOs are no longer symmetry adapted (see the text for details).
[c]These results were obtained using four references (see footnote b) and two-configurational MCSCF orbitals.

only briefly point out the main differences between these two approaches and refer the reader for details to the above given reviews and to the original literature.[20,23–31] The general SU CCSD equations have the form[20]

$$\langle G_l(i)\Phi_i|e^{-T(i)}He^{T(i)}|\Phi_i\rangle = \sum_{j(\neq i)} \langle G_l(i)\Phi_i|e^{-T(i)}e^{T(j)}|\Phi_j\rangle H_{ji}^{(\mathrm{eff})}, \quad (3)$$

where $H_{ji}^{(\mathrm{eff})}$ designates the matrix elements of the effective Hamiltonian and the use of the complete model space (CMS) is assumed. When using a GMS, special precautions are required, namely, the so-called C-conditions for the internal amplitudes.[95–98] Since the model space employed in the present calculations is a CMS, the C-conditions are not required. Finally, in the SU CCSD(T) method,[99] the triples are accounted for via a perturbative correction of diagonal matrix elements of the effective Hamiltonian.

In the SS (or Mk) CCSD method,[24–29] a different set of equations is solved for each state considered (even though most applications focus on only the lowest state of a given symmetry species). For the αth state, the working equations can be cast into a form similar to that of the above given SU CC equations, namely,

$$\langle G_l(i)\Phi_i|e^{-T(i)}He^{T(i)}|\Phi_i\rangle = -\sum_{j(\neq i)} \langle G_l(i)\Phi_i|e^{-T(i)}e^{T(j)}|\Phi_i\rangle H_{ij}^{(\mathrm{eff})}(c_{j\alpha}/c_{i\alpha}). \quad (4)$$

The working equations of the SU and SS methods thus differ in the form of the coupling terms.

The main advantage of the SS approach stems from the fact that, as in the BW CCSD method, when focusing on a single state at a time, the intruder state problem is much less likely to occur. On the other hand, each state requires a repeated solution of essentially the same set of equations, while in the standard SU approach all states are considered simultaneously in the true spirit of MR-type formalism. However, the genuine SU approach will suffer once intruder states intervene, in which case the SS approach must be preferred. We shall attempt to compare the main results as rendered by these two, as well as BW MRCC methods, wherever available.

III. ORBITAL ROTATION INVARIANCE OF RMR CCSD

As already pointed out, the RMR CCSD and RMR CCSD(T) methods,[50,60,61] as well as their performance,[14,64–66,84–94] have been amply documented in the literature. While the minor violation of size extensivity was tested for a number of situations (see, e.g., Ref. 47), no investigation of the invariance of this approach with respect to the orbital rotation has been documented. We thus wish to illustrate this aspect employing CBD as an example, using a simple Dunning–Hay basis.[100] For this purpose we designate molecular orbitals (MOs) 1–13 as the occupied ones, 14th and 15th orbitals as active MOs, and all higher-lying ones as virtual MOs. The results involving rotations of occupied, virtual, and active MOs are given in Table I. In these calculations, we mix two occupied or two virtual orbitals that belong to the same or to different symmetries.

We first recall that CCSD is fully invariant with respect to both the occupied-occupied and virtual-virtual rotations (see Table I), while the CCSD(T) method is not, since such rotations generally lead to noncanonical orbitals. However, the invariance property may be recovered if the T_3 amplitudes are obtained iteratively (see Ref. 101). The results given in Table I indicate that when the rotation involves only valence-shell orbitals, the invariance property is to a large degree maintained even in CCSD(T), the noninvariance effects being at a microhartree level. However, when the rotation involves a 1s orbital on carbon and a valence-shell orbital (orbitals 1 and 5 in Table I), namely, the two orbitals whose orbital energies are significantly different, the effect due to the rotation is at the 0.1 mE_h level.

The invariance characteristics of RMR CCSD and RMR CCSD(T) are similar to those of CCSD and CCSD(T): RMR CCSD is invariant with respect to the occupied-occupied and virtual-virtual rotations while RMR CCSD(T) is not invariant and the effects are of the same order of magnitude as for

CCSD(T), i.e., very small if we mix only valence-shell orbitals. When we consider a rotation of the two active orbitals (belonging to the b_{1g} and b_{2g} symmetry species), we encounter a more complex situation. Within the SR CC framework this amounts to the mixing of the occupied and virtual MOs, so that even CCSD is not invariant. Neither is the two-reference (2R) RMR CCSD in which case the rotation effect is of the order of 0.4 mE_h. Of course, this rather large effect arises because we rotate two active orbitals belonging to distinct symmetry species, so that the resulting active MOs are no longer symmetry adapted, calling for a four-reference (4R) CMS. Indeed, with 4R RMR CCSD this effect reduces to -0.015 mE_h when using restricted Hartree-Fock (RHF) orbitals and to -0.022 mE_h when we employ two-configurational SCF orbitals. Here we must point out that the effect of active-active orbital rotation on MkCCSD energy amounts to -3.228 mE_h, according to Ref. 80 (though, we must note that the RMR and MkCC calculations are not entirely equivalent, since they use different basis sets and geometries).

We can thus conclude that the RMR CCSD is fully invariant with respect to the occupied-occupied and virtual-virtual orbital rotations. With perturbative triple corrections, RMR CCSD(T) behaves similarly as the standard SR CCSD(T) and its invariance can be achieved if the T_3 amplitudes are obtained iteratively. With respect to the active-active orbital rotations, RMR CCSD is not invariant, yet the effect is rather small, assuming that we use a CMS.

IV. COMPUTATIONAL DETAILS

We employ cc-pVDZ, cc-pVTZ, and cc′-pVTZ basis sets[102] (the prime indicates that the *f* functions on carbon and the *d* functions on hydrogen are deleted) and we freeze 1*s* orbitals on carbon in all correlated calculations. In addition, we also employ the STO-3G basis set, in which case we are able to carry out FCI calculations correlating 12 electrons in 18 MOs (freezing 1*s* and 2*s* orbitals on carbon). Since these results represent the exact solution for the chosen *ab initio* model, they are helpful in assessing the performance of various MR CC methods.

Most studies of the automerization of CBD first optimize the rectangular and square geometries and calculate their energies. However, such an approach does not reveal the details of the automerization potential in the whole range of geometries. We thus prefer to employ a simple one-parameter model by requiring the sum of the long and short bond lengths to have a constant value, equal to twice the bond length of the optimized square geometry configuration. We thus explore the cut of the PES as a function of the bond-length parameter $R \equiv R_1$ with the second bond length R_2 given by $R_2 = 2R_0 - R$. Although for the exactly optimized geometries the average bond length $(R_1+R_2)/2$ of the rectangular structure slightly deviates from the equilibrium square configuration bond length R_0, this deviation is very small (e.g., in the case of the AQCC/SA-4-CASSCF result[78] with the cc-pVTZ basis set, it amounts to less than 0.01 Å). Thus, in all figures we employ the RMR CCSD(T)/cc-pVDZ value of $R_0 = 1.4668$ Å, fix the C–H bond length at 1.079 Å, and the HCC bond angle at 135°.

In the square geometry both reference configurations are exactly degenerate and have the same weight in the resulting wave functions. In a rectangular conformation, one reference configuration is dominant, yet the weight of the second configuration is still quite significant, amounting to about 0.2. For this reason in all our MR CC calculations we employ a 2R approach.

Concerning the notation, we employ the acronym MkCCSD for the SS version of the SU MRCC method as introduced by Mukherjee and co-workers,[23–31] since the acronym SS CCSD has been used for several other SS-type approaches (cf., e.g., Refs. 103 and 104).

We employ the IAM (Ref. 83) to compute the energy of the zero and the first vibrational levels for each vibrational mode, whose difference yields the corresponding fundamental frequency. This involves a solution of the pertinent integral equation, which is supplemented by the second order perturbative approach providing improved results. The required normal mode coordinates are obtained first at the RHF/cc-pVDZ level and are subsequently used in generating the appropriate cut of the PES along each normal coordinate. The original purpose of the IAM algorithm[83] was to overcome anomalies in the potential that is based on post-Hartree–Fock approaches using unstable RHF or restricted open-shell HF (ROHF) wave functions as a reference. In such cases the approaches based on the evaluation of the second derivatives are unreliable. Although in the case of a rectangular CBD the computed potentials do not display any irregularity, the use of the IAM approach is nonetheless useful, since it implicitly accounts for the anharmonicity by generating the fundamental, rather than harmonic, frequencies. In labeling the vibrational modes we follow the convention used for experimental frequencies,[72,105] which assumes the molecular plane to be defined by the *yz* coordinates. Note, however, that some authors (see, e.g., Ref. 78) identify the *xy* plane with the molecular plane.

Our recent implementation of the MkCCSD (or SS CCSD) method is based on our GMS SU CC codes. All SR and MR CC calculations presented here have been carried out with our own codes, which interface with GAMESS.[106] The GAMESS package has also been used to perform the MCSCF, MP2 (second-order MBPT), FCI, and CR-CC(2,3) (cf. Refs. 43–45) calculations.

V. RESULTS AND DISCUSSION

A. The FCI/STO-3G model

Since FCI represents the exact solution for a given *ab initio* model as defined by the basis set employed, it can serve as an absolute benchmark for a comparison with all other approximate methods. Using the STO-3G basis and correlating 12 electrons (see Sec. IV), we compute the FCI potential energy for a series of *R* values and show the deviations from these FCI values for the SR CCSD(T), SU CCSD, MkCCSD, RMR CCSD, and RMR CCSD(T) methods in Table II (the corresponding reference RHF, MCSCF, and FCI

TABLE II. Deviations ΔE from the FCI energies, $\Delta E=E-E(\mathrm{FCI})$ (in mE_h), for the automerization of cyclobutadiene, as obtained with various CC methods, STO-3G basis set, and RHF orbitals, correlating 12 electrons in 18 MOs. The automerization pathway is defined by the shorter bond length R (in Å) of a rectangular conformation, keeping the sum of the shorter and longer bond lengths equal to twice the equilibrium bond length of a square conformation (1.4668 Å). The maximal and minimal deviations from FCI, as well as the NPE, are also indicated. At the bottom of the table we also list these deviations and NPE for the case when the MCSCF orbitals are used. For the sake of completeness, we also list the corresponding RHF, MCSCF, and FCI energies in a supplementary material to this paper (Ref. 107).

R (Å)	CCSD(T)	SU CCSD	MkCCSD	RMR CCSD	RMR CCSD(T)
1.2668	0.734	1.304	2.344	1.899	0.323
1.3168	0.857	0.950	2.213	1.860	0.323
1.3468	0.948	0.664	2.107	1.878	0.339
1.3568	0.977	0.550	2.061	1.895	0.349
1.3668	1.002	0.422	2.007	1.919	0.363
1.3768	1.018	0.281	1.946	1.952	0.381
1.3868	1.019	0.120	1.875	1.998	0.405
1.4068	0.918	−0.256	1.697	2.145	0.477
1.4168	0.760	−0.470	1.591	2.257	0.527
1.4268	0.457	−0.693	1.478	2.405	0.588
1.4368	−0.098	−0.911	1.365	2.594	0.653
1.4468	−1.078	−1.100	1.265	2.823	0.704
1.4568	−2.750	−1.234	1.193	3.079	0.705
1.4668	−5.466	−1.287	1.165	3.326	0.593
ΔE(min)	−5.466	−1.287	1.165	1.860	0.323
ΔE(max)	1.019	1.304	2.344	3.326	0.705
NPE	6.485	2.591	1.179	1.465	0.383
			Using MCSCF orbitals		
ΔE(min)		−1.292	1.170	1.837	0.233
ΔE(max)		1.176	2.238	3.425	0.688
NPE		2.468	1.068	1.588	0.455

energies are listed in Table I of the supplement;[107] note also that the FCI calculations involve only valence orbitals and keep core orbitals frozen as explained in greater detail in the supplement[107]). For an easy overall assessment we also give the maximal and minimal deviations, as well as the nonparallelism error (NPE). We recall that the NPE is defined as the difference between the maximal and minimal deviations from the FCI energies and indicates the degree of parallelism with the FCI PEC. The maximum and minimum deviations and the NPE are also presented for the case when we employ MCSCF MOs. In the entire range of geometries considered the NPE of SU CCSD is 2.591 mE_h, while the corresponding value for MkCCSD is 1.179 mE_h, a definite improvement over the standard SU CCSD. The RMR CCSD NPE of 1.465 mE_h lies in between these values. However, when corrected for secondary triples, the NPE of RMR CCSD(T) is 0.383 mE_h, representing by far the best result, not to mention the standard SR CCSD(T), which is inferior to all other approaches used with NPE of 6.485 mE_h. When we use the two-configurational MCSCF orbitals in lieu of the RHF ones, we obtain qualitatively the same results.

We also observe that the SU CCSD energies are always lower than the MkCCSD ones. In fact, at the square geometry, the SU CCSD energy lies below the FCI value. On the whole, the SU CCSD and MkCCSD potentials are roughly "parallel" and their relative NPE amounts to only 1.4 mE_h for the entire range of geometries considered. This is also the case when we use the cc-pVDZ basis, in which case the MkCCSD and SU CCSD potentials have a relative NPE of 1.68 and 1.50 mE_h when using the RHF and MCSCF MOs, respectively. Again, the SU CCSD energies are always lower than the MkCCSD ones. We can thus conclude that, for all practical purposes, SU CCSD and MkCCSD yield essentially equivalent results.

B. The automerization potentials

The automerization potentials at the SD-level of approximation that are based on a one-parameter model described in Sec. IV, as obtained with the cc-pVDZ basis and the equilibrium square geometry bond length $R_0=1.4668$ Å, using the RHF and MCSCF MOs, are shown in Figs. 1 and 2, respectively. Analogous results, perturbatively corrected for triples, are then shown in Fig. 3.

It is a well-known fact that at the square geometry the RHF wave functions represent a broken symmetry solution. Two such equivalent and degenerate solutions coexist at the square geometry and the corresponding potentials form a crossing node[108] (or c-node; see the insert in Fig. 1). These solutions correspond to the two possible valence bond structures. In contrast, the MCSCF orbitals and the energy change smoothly from one rectangular geometry to another (see the insert in Fig. 2).

The results in Fig. 1 clearly indicate how the symmetry breaking at the RHF level proliferates even to the CCSD correlated level. In contrast, for genuine MR CC approaches

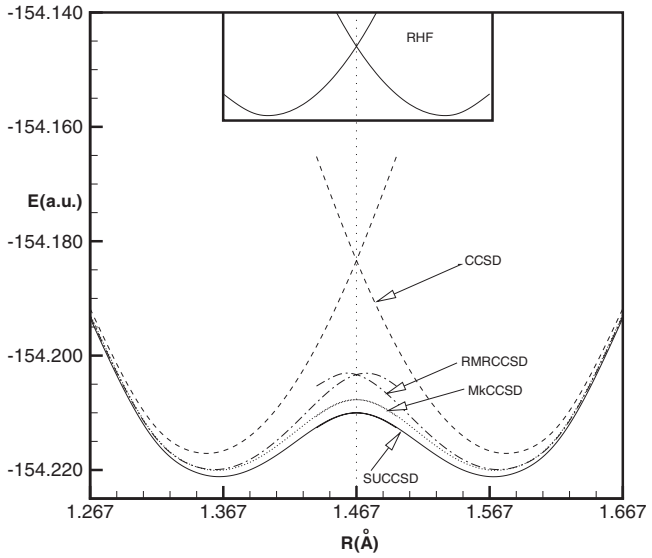

FIG. 1. The automerization potential of cyclobutadiene obtained with CCSD and various MR CCSD methods employing RHF orbitals and a cc-pVDZ basis set. One C–C bond length is labeled by $R_1 \equiv R$ and the other one is given by $R_2 = 2 \times 1.4668 - R$ (all bond-length values are in angstroms). A representation of the potential obtained with the two RHF solutions is shown in the insert.

of both the SU CCSD and MkCCSD kind, the effect of symmetry breaking at the square geometry is very small and hardly visible on the scale of the figure. However, this effect is much larger in the case of RMR CCSD, when the apex of the potential does not occur at the square geometry (cf. Fig. 3). This deficiency disappears once we employ MCSCF orbitals (cf. Fig. 2) when the effect due to the c-node in the reference potential is hardly discernible, even in the case of the RMR CCSD potential and, of course, also for the SU CCSD and MkCCSD potentials.

It is not surprising that the noniterative, perturbative triple (T)-correction, that relies on the SR MBPT and RHF MOs, has a tendency to emphasize the shortcomings due to the symmetry breaking at the RHF level (cf. Fig. 3), causing

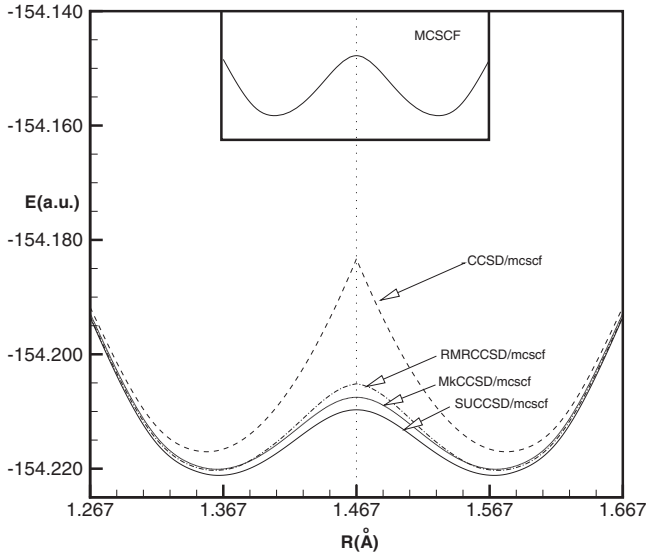

FIG. 2. Same as Fig. 1 but using two-configurational MCSCF orbitals. A representation of the MCSCF potential is again shown in the insert.

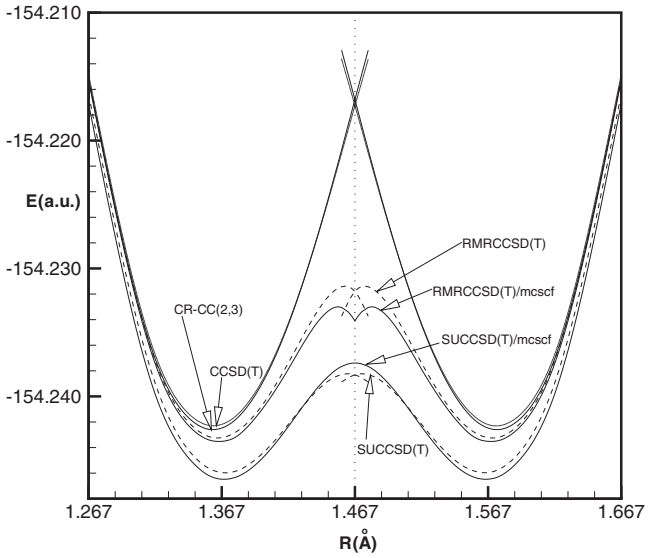

FIG. 3. Same as Figs. 1 and 2, but using various CC methods perturbatively corrected for triples. See the text for details.

a small dip, and a consequent singular behavior, in the vicinity of the square geometry. Again, this effect is more pronounced in the RMR CCSD(T) case than in the SU CCSD(T) potential. In the RMR case, the use of the MCSCF orbitals is not helpful, since in the SR MBPT, the Fock matrix is diagonal, which is no longer the case when the orbitals are replaced by the MCSCF ones. However, the use of the MCSCF MOs is helpful in the case of SU CCSD(T).

In order to provide a more quantitative characterization of the above mentioned behavior, we computed the right-hand and left-hand slopes (for $R < 1.4668$ Å and $R > 1.4668$ Å) at R_0. In the ideal case, both of these derivatives should be identical and vanish. When we employ MCSCF orbitals, these derivatives are smaller than 10^{-7} for RMR CCSD, SU CCSD, and MkCCSD (with energies in a.u. and the bond length R in angstroms). When we employ RHF MOs, these derivatives only slightly deviate from zero, being $\sim 5 \times 10^{-7}$ in the case of SU CCSD and $\sim 1.2 \times 10^{-5}$ for RMR CCSD. However, once the perturbative (T)-corrections are implemented, the magnitude of these derivatives increases to $\sim 5 \times 10^{-6}$ for SU CCSD(T) and $\sim 2.2 \times 10^{-5}$ for RMR CCSD(T). For the sake of comparison, the value for the CCSD(T) potential is $\sim 7 \times 10^{-5}$.

A surprising result is rendered by the CR-CC(2,3) method,[43–45] which is generally very effective in overcoming the shortcomings of the standard CCSD(T) method. In the present situation, however, this approximation does not provide a meaningful improvement over CCSD(T). The reason for this behavior is likely the fact that in this case the quadruples play a very significant role, so that CR-CC(2,3), generally representing an excellent approximation to SR CCSDT, does not suffice. This also emphasizes the fact that the CBD problem represents a genuine MR case, requiring a genuine MR approach.

C. Frequencies

The computed frequencies for rectangular CBD are listed in Table III. Since the rectangular CBD ground state is

TABLE III. Computed (using a cc′-pVTZ basis set) fundamental vibrational frequencies $\nu_1-\nu_0$ (in cm^{-1}) of cyclobutadiene and a comparison with the experimental and literature values.

Sym.[a]	No.	CCSD	CCSD(T)	RMR CCSD	RMR CCSD(T)	Ref. 73	Ref. 78	Exp.[b]
a_g	1	3245	3233	3246	3234	3206	3263	3140
	2	1570	1502	1508	1455[c]	1469	1489	1678
	3	1136	1119	1130	1114	1113	1119	1059
	4	960	940	940	927	925	921	989
b_{1g}	1	830	781	811	770	776	802	
b_{2g}	1	561	511	560	507	540	540	531
b_{3g}	1	3213	3204	3214	3206	3157	3213	3093
	2	1196	1175	1197	1175	1145	1184	
	3	879	867	887	870	867	873	723
a_u	1	789	734	780	732	754	767	
	2	554	527	547	520	509	501	
b_{1u}	1	3246	3239	3244	3238	3195	3249	3124
	2	1523	1501	1497	1494	1542	1545	1527
	3	1051	1035	1048	1033	1023	1050	1028
b_{2u}	1	3230	3222	3228	3220	3178	3230	3105
	2	1290	1267	1285	1265	1253	1276	1244
	3	757	730	742	722	760	706	719
b_{3u}	1	604	569	590	550	577	564	576

[a]The same symmetry labeling as in Refs. 72 and 105 is used. It corresponds to a choice of the yz plane as the molecular plane. Note that some authors (e.g., Ref. 78) identify the molecular plane with the xy plane, resulting in a different symmetry labeling.
[b]From Refs. 72 and 105.
[c]This frequency attains the value of 1483 cm^{-1} when we use the MP2/cc-pVTZ geometry instead of the RMR CCSD(T)/cc-pVDZ one (see the text).

quasidegenerate (the amplitude of the most important doubly excited configuration being about 0.2), we computed the frequencies using the RMR CCSD and RMR CCSD(T) potentials, as well as, for the sake of a comparison, using the SR CCSD and CCSD(T) potentials. In all cases we employed RMR CCSD(T)/cc-pVDZ geometry. In Table III, the resulting fundamental frequencies, obtained via the IAM procedure, are also compared with both the experimental values[72,105] and available theoretical results.[73,78]

The computed fundamental frequencies are obtained as a difference between the first- and the zero-vibrational levels. Both the cc-pVDZ and cc′-pVTZ basis sets were employed, but only the results obtained with the latter basis are presented in Table III. In general, a larger basis set improves the frequencies for the C–H stretching modes that exceed 3000 cm^{-1} by about 100–170 cm^{-1}. For most of the other modes the improvements are modest. Note that we label the frequencies by their symmetry and by the sequential number according to their decreasing value (identifying the molecular plane with the yz plane).

We find a very good overall agreement between the computed and experimental frequencies, yet even better one between our results and those obtained by other authors. The average absolute deviation between our frequencies and those of Refs. 73 and 78 (cf. Table III) amounts to only 23.3 and 17.4 cm^{-1}, respectively, while the average signed deviations are −3.9 and 12.8 cm^{-1}. Remarkably, the largest discrepancies generally occur for those modes for which we find significant anharmonicities, as implied by the results given in Table III (see below).

By far the largest discrepancy between the computed and experimental frequencies (195 cm^{-1}) is found for the second a_g mode (cf. a_g-2 mode frequencies in Table III). This frequency is also most influenced by the MR nature of the CBD ground state (as measured by the difference between the RMR CCSD and CCSD values). At the CCSD level, this effect amounts to −62 cm^{-1}. The CCSD(T) and RMR CCSD(T) values are, respectively, 1502 and 1455 cm^{-1}. The latter value is, however, rather sensitive to the equilibrium geometry employed and becomes 1483 cm^{-1} when we use the MP2/cc-pVTZ geometry (cf. Table III). The reason for this behavior is easy to see. As mentioned above, the amplitude of the largest doubly excited configuration is about 0.2 and, for most vibrational modes, the weight of this configuration remains roughly constant when the nuclear framework is distorted due to the vibrational motion. However, in the case of the a_g-2 mode, the amplitude of this configuration undergoes a significant change from 0.18 at $\delta q=0.20$ a.u. to 0.25 at $\delta q=-0.20$ (δq being the displacement along the a_g-2 normal mode). This represents the largest change of all the modes concerned.

Now, when compared with experiment, an account of the MR effects leads to a less satisfactory agreement, especially for the a_g-2 mode. In general, the CCSD and CCSD(T) frequencies are closer to the experimental values than are the RMR CCSD and RMR CCSD(T) ones. Yet, the RMR CCSD, and particularly the RMR CCSD(T), frequencies for the a_g-2 mode agree very well with other theoretical results[73,78] (differing by 14 and 6 cm^{-1}, respectively). Moreover, using a different equilibrium geometry leads to only an insignificant change in this frequency (recall the above mentioned results obtained with the RMRCCSD(T)/cc-pVDZ geometry and MP2/cc-pVTZ geometry). We thus do not understand why the discrepancy with experiment increases when we account

TABLE IV. Comparison of harmonic frequencies (ω), zero-energy levels (ν_0), and differences between the first- and the zero-energy levels ($\Delta\nu=\nu_1-\nu_0$) of cyclobutadiene. The last two columns compare the harmonic and anharmonic approximations. All values are in cm^{-1} and are based on the MP2/cc-pVTZ potential

Sym.	No.	ω	ν_0	$\Delta\nu$	$2\nu_0-\omega$	$\Delta\nu-\omega$
a_g	1	3275	1647	3261	19	−14
	2	1561	787	1566	14	5
	3	1125	564	1127	2	2
	4	973	487	972	1	−1
b_{1g}	1	860	438	887	16	27
b_{2g}	1	578	306	636	33	58
b_{3g}	1	3230	1641	3277	52	47
	2	1204	604	1208	4	4
	3	853	426	852	−1	−1
a_u	1	844	430	877	17	33
	2	523	262	526	2	3
b_{1u}	1	3266	1658	3311	51	45
	2	1572	795	1589	18	17
	3	1068	534	1069	0	1
b_{2u}	1	3244	1648	3290	52	46
	2	1273	638	1275	3	2
	3	724	366	732	7	8
b_{3u}	1	576	304	631	31	55

for quasidegeneracy of the state considered, except the possibility that the experimental value is too high.

To assess more explicitly the role of anharmonicity we employed the MP2/cc-pVTZ potentials. In this case the geometry was fully optimized at the same MP2/cc-pVTZ level of theory and the harmonic frequencies were computed using the analytical Hessian approach. Subsequently, the MP2 potentials were generated for each normal mode and used to computed the zero- and the first-vibrational levels via the IAM procedure, yielding the fundamental frequencies. These results are presented in Table IV. The anharmonicities are found to be larger for the C–H stretching modes (whose frequencies are larger than 3000 cm^{-1}) and for the out-of-plane [OPLA (Ref. 105)] modes (b_{1g}-1, b_{2g}-1, a_u-1, and b_{3u}-1). The potentials for the OPLA modes are often too flat at the equilibrium geometry and the computed fundamental frequencies are larger than the harmonic frequencies.

D. Barrier height

An accurate determination of the barrier height for the CBD automerization was not the aim of this study. Nonetheless, we can compute the barrier height along the one-parameter stretching mode R considered above, yielding the results listed in Table V. The results obtained with the cc-pVTZ basis set used the RMR CCSD(T)/cc-pVDZ geometries. These results are also compared with those available in the literature. Very recent results obtained with various SS equation of motion CCSD methods[79] yield slightly elevated values, ranging from 9.5 to 10.3 kcal/mol, but still within the range of experimental values (these results are not included in Table V).

The results employing cc-pVTZ basis yield generally a larger barrier height than do those using the cc-pVDZ basis. A further increase in the size of the basis set beyond cc-pVTZ could increase these values by an additional ~0.4 kcal/mol (see Ref. 78). The results obtained with the MCSCF orbitals should also be more reliable than those employing RHF MOs, since they provide a better description in the vicinity of the square geometry.

Finally, the adjustment for the zero-point vibrational energy (ΔZPVE) that is required when we wish to make a comparison with experiment represents a sizable correction. Different estimates[73,78] indicate that ΔZPVE is about −2.5 kcal/mol, which must be added to the electronic energy differences to get the value that can be compared with experiment. Unfortunately, the experimental values for the barrier height spread over a rather wide range of 1.6–10 kcal/mol.[67,68] The RMR CCSD(T)/cc-pVTZ value (using MCSCF orbitals) when corrected for the ΔZPVE is ~5 kcal/mol, which is in the middle of the range of experimental values. We note that a recent study[78] based on the MR AQCC calculations recommends the value of 6.3 kcal/mol as "the best estimate" for the barrier height. Considering that the value obtained by Balková and Bartlett[73] (when corrected for ΔZPVE) is lower than the above mentioned best estimate benchmark by 2.3 kcal/mol, our results are very close to the average of these two estimates.

VI. CONCLUSIONS

We investigated the automerization of CBD to examine the effectiveness of the RMR-type methods in accounting for the MR nature of the states involved, since the employed model involves various degrees of quasidegeneracy along the automerization pathway. In fact, even the equilibrium rectangular geometry possesses a significant MR character, which steadily increases as we approach the square geometry, in which case we have to deal with a complete degeneracy and the associated singular behavior of the RHF reference that generally propagates to the post-Hartree–Fock correlated level. This is indeed the case for RMR-type methods, which

TABLE V. Barrier heights (in kcal/mol) for the automerization of cyclobutadiene (using square geometry with $R_1=R_2=1.4668$ Å and the rectangular geometry obtained by optimizing R_1 while $R_1+R_2=2\times1.4668$ Å in each case, see the text for details.)

	Barrier (kcal/mol)	
Method	cc-pVDZ	cc-pVTZ[a]
CCSD	21.2	
SUCCSD	7.0	8.7
MkCCSD	7.8	9.6
RMRCCSD	10.4	13.0
CCSD(T)	15.7	
SUCCSD(T)	4.8	5.9
RMRCCSD(T)	7.2	9.5
SUCCSD/mcscf	7.2	8.9
MkCCSD/mcscf	7.9	9.7
RMRCCSD/mcscf	9.5	11.4
SUCCSD(T)/mcscf	5.7	7.2
RMRCCSD(T)/mcscf	5.9	7.5
CCSDT[b]	6.4	
2D-MRCCSD(T)[b]	6.6	
BWCCSD (a.c.)[c]	6.5	7.6
BWCCSD (i.c.)[c]	6.2	7.4
BWCCSD(T) (a.c.)[c]	6.1	7.0
BWCCSD(T) (i.c.)[c]	5.7	6.8
MkCCSD[c]	7.8	9.1
MkCCSD(T)[c]	7.8	8.9
AQCC/SA-2-CASSCF[d]	7.3	8.4
ΔZPVE [e]	−2.5	

[a]These results employed RMR CCSD(T)/cc-pVDZ geometries.
[b]Reference 73, using a split-valence [3s2p1d/1s] basis.
[c]Reference 80; a.c. indicates an additive correction for size-extensivity and i.c. an iterative correction.
[d]Reference 78.
[e]ΔZPVE (zero-point vibrational energy) correction as estimated in Ref. 78.

represents essentially a SR CCSD approach that is corrected for the most important three- and four-body cluster amplitudes, so that the singularity of the RHF MOs leads generally to an anomalous behavior of the potentials in the vicinity of the square geometry. In this context it is interesting to explore the effect of using the MCSCF MOs, which very significantly rectify the computed PECs.

A comparison of the resulting potentials with the FCI ones (Table II) reveals that, at least at the SD level, the MkCCSD method is superior to both the SU CCSD and RMR CCSD approaches when measured by the NPE values, regardless which MOs are employed. Only when RMR CCSD is corrected for the secondary triples do we generate very much superior RMR CCSD(T) potential, except perhaps in the immediate vicinity of the square geometry. Of course, all these MR-type approaches yield vastly superior results to the standard CCSD(T) method, as indicated by both the maximum deviations from the FCI energies and by the NPE values for the relevant range of R values from 1.2668 to 1.4668 Å. Interestingly enough, while the MCSCF MOs yield much smoother RMR CCSD potential in the vicinity of the square geometry than do the RHF MOs (cf. Figs. 1 and 2), this behavior is not reflected in the NPEs at the FCI/STO-3G level, which in fact slightly deteriorates when using MCSCF MOs.

It is also gratifying that, on the whole, the RMR CCSD(T)/cc′-pVTZ fundamental frequencies agree rather well with theoretical results that were independently generated by other authors.[73,78] On the average, our frequencies are slightly larger (by ~4 cm^{-1}) than the TD-CCSD (i.e., 2R SU CCSD) ones of Balková and Bartlett,[73] and slightly smaller (by ~13 cm^{-1}) than the AQCC values of Eckert-Maksić *et al.*,[78] although, measured by the mean square deviations, the latter ones are closer to ours (~17 versus ~23 cm^{-1}; see Sec. V C and Table III for details). While the agreement with other theoretical results is remarkably good, the agreement with the experimental values is slightly worse, though still remarkably good considering the circumstances. Moreover, as already pointed out earlier, the largest discrepancies seem to occur for frequencies characterized by relatively large anharmonicities, as theoretically estimated using the MP2 potentials. This agreement also corroborates the validity and performance of the IAM that has been employed in the computing of our fundamental frequencies. Likewise, we obtain a very satisfactory value for the automerization barrier height that represents an arithmetic average of the two other[73,78] theoretical values and lies in the middle of the range of experimental values.

We can thus conclude that the RMR CCSD(T) method represents a valuable tool that is capable to properly account even for very strong quasidegeneracies, while also performing well in nondegenerate situations, where it becomes practically identical with the standard SR CCSD(T). This is certainly the case when quadruples are not negligible, in which case the RMR methods clearly outperform the SR-based CCSD approaches, including CCSD(T). We note, finally, that in the case of the genuine MR CC methods, of either the SU or SS variety, a rigorous perturbation theory justification of the (T) correction is rather unsatisfactory, while in the RMR CCSD(T) case it is, in general, reasonably well justified, since those triples that are large enough to cause the breakdown of the standard CCSD(T) are accounted for independently as primary triples via external correction of CCSD equations.

ACKNOWLEDGMENTS

The continued support (J.P.) by the Natural Sciences and Engineering Research Council of Canada (Grant No. RGPIN5806-05) is gratefully acknowledged

[1] J. Čížek, J. Chem. Phys. **45**, 4256 (1966).
[2] J. Čížek, Adv. Chem. Phys. **14**, 35 (1969).
[3] J. Paldus, J. Čížek, and I. Shavitt, Phys. Rev. A **5**, 50 (1972).
[4] G. D. Purvis III and R. J. Bartlett, J. Chem. Phys. **76**, 1910 (1982).
[5] K. Raghavachari, G. W. Trucks, J. A. Pople, and M. Head-Gordon, Chem. Phys. Lett. **157**, 479 (1989).
[6] R. J. Bartlett, in *Modern Electronic Structure Theory, Part I*, edited by D. R. Yarkony (World Scientific, Singapore, 1995), pp. 1047–1131.
[7] J. Gauss, in *Encyclopedia of Computational Chemistry*, edited by P. von R. Schleyer (Wiley, New York, 1998), Vol. 1, pp. 615–636.
[8] J. Paldus and X. Li, Adv. Chem. Phys. **110**, 1 (1999).
[9] J. Paldus, in *Handbook of Molecular Physics and Quantum Chemistry*, edited by S. Wilson (Wiley, Chichester, 2003), Vol. 2, Chap. 19, pp. 272–313.
[10] T. D. Crawford and H. F. Schaefer III, in *Reviews in Computational Chemistry*, edited by K. B. Lipkowitz and D. B. Boyd (Wiley, New York, 2000), Vol. 14, Chap. 2, pp. 33–136.

[11] R. J. Bartlett and M. Musiał, Rev. Mod. Phys. **79**, 291 (2007).
[12] J. Paldus, in *Theory and Applications of Computational Chemistry: The First Forty Years*, edited by C. E. Dykstra, G. Frenking, K. S. Kim, and G. E. Scuseria (Elsevier, Amsterdam, 2005), Chap. 7, pp. 115–147.
[13] R. J. Bartlett, in *Theory and Applications of Computational Chemistry: The First Forty Years*, edited by C. E. Dykstra, G. Frenking, K. S. Kim, and G. E. Scuseria (Elsevier, Amsterdam, 2005), Chap. 42, pp. 1191–1221.
[14] X. Li and J. Paldus, J. Chem. Phys. **129**, 054104 (2008).
[15] X. Li and J. Paldus, Chem. Phys. Lett. **431**, 179 (2006).
[16] X. Li, J. R. Gour, J. Paldus, and P. Piecuch, Chem. Phys. Lett. **461**, 321 (2008).
[17] I. Lindgren, Int. J. Quantum Chem., Quantum Chem. Symp. **12**, 33 (1978).
[18] I. Lindgren and D. Mukherjee, Phys. Rep. **151**, 93 (1987).
[19] B. Jeziorski and J. Paldus, J. Chem. Phys. **90**, 2714 (1989).
[20] B. Jeziorski and H. J. Monkhorst, Phys. Rev. A **24**, 1668 (1981).
[21] J. Paldus, in *Methods in Computational Molecular Physics*, NATO ASI Series B: Physics No. 293, edited by S. Wilson and G. H. F. Diercksen (Plenum, New York, 1992), pp. 99–194.
[22] J. Paldus, in *Relativistic and Electron Correlation Effects in Molecules and Solids*, NATO ASI Series B: Physics No. 318, edited by G. L. Malli (Plenum, New York, 1994), pp. 207–282.
[23] F. A. Evangelista, W. D. Allen, and H. F. Schaefer III, J. Chem. Phys. **125**, 154113 (2006).
[24] U. S. Mahapatra, B. Datta, B. Bandyopadhyay, and D. Mukherjee, Adv. Quantum Chem. **30**, 163 (1998).
[25] U. S. Mahapatra, B. Datta, and D. Mukherjee, J. Chem. Phys. **110**, 6171 (1999).
[26] S. Chattopadhyay, U. S. Mahapatra, and D. Mukherjee, J. Chem. Phys. **112**, 7939 (2000).
[27] S. Chattopadhyay, D. Pahari, D. Mukherjee, and U. S. Mahapatra, J. Chem. Phys. **120**, 5968 (2004).
[28] S. Chattopadhyay, P. Ghosh, and U. S. Mahapatra, J. Phys. B **37**, 495 (2004).
[29] U. S. Mahapatra, B. Datta, and D. Mukherjee, in *Recent Advances in Coupled Cluster Methods*, edited by R. J. Bartlett (World Scientific, Singapore, 1997), pp. 155–181.
[30] F. A. Evangelista, W. D. Allen, and H. F. Schaefer III, J. Chem. Phys. **127**, 024102 (2007).
[31] F. A. Evangelista, A. C. Simmonett, W. D. Allen, H. F. Schaefer III, and J. Gauss, J. Chem. Phys. **128**, 124104 (2008).
[32] I. Hubač and P. Neogrády, Phys. Rev. A **50**, 4558 (1994).
[33] J. Mášik, I. Hubač, and P. Mach, J. Chem. Phys. **108**, 6571 (1998).
[34] J. Pittner, P. Nachtigall, P. Čársky, J. Mášik, and I. Hubač, J. Chem. Phys. **110**, 10275 (1999).
[35] I. Hubač, J. Pittner, and P. Čársky, J. Chem. Phys. **112**, 8779 (2000).
[36] J. Pittner, J. Chem. Phys. **118**, 10876 (2003).
[37] J. Pittner and O. Demel, J. Chem. Phys. **122**, 181101 (2005).
[38] J. Pittner, X. Li, and J. Paldus, Mol. Phys. **103**, 2239 (2005).
[39] J. Brabec and J. Pittner, J. Phys. Chem. **110**, 11765 (2006).
[40] K. Kowalski and P. Piecuch, J. Chem. Phys. **113**, 18 (2000).
[41] K. Kowalski and P. Piecuch, J. Chem. Phys. **115**, 2966 (2001).
[42] K. Kowalski and P. Piecuch, J. Chem. Phys. **122**, 074107 (2005) (and references therein).
[43] P. Piecuch and M. Włoch, J. Chem. Phys. **123**, 224105 (2005).
[44] P. Piecuch, M. Włoch, J. R. Gour, and A. Kinal, Chem. Phys. Lett. **418**, 467 (2006).
[45] M. Włoch, J. R. Gour, and P. Piecuch, J. Phys. Chem. A **111**, 11359 (2007).
[46] X. Li and J. Paldus, J. Chem. Phys. **128**, 144118 (2008).
[47] X. Li and J. Paldus, J. Chem. Phys. **128**, 144119 (2008).
[48] J. Paldus and J. Planelles, Theor. Chim. Acta **89**, 13 (1994).
[49] L. Z. Stolarczyk, Chem. Phys. Lett. **217**, 1 (1994).
[50] J. Planelles, J. Paldus, and X. Li, Theor. Chim. Acta **89**, 33 (1994).
[51] J. Planelles, J. Paldus, and X. Li, Theor. Chim. Acta **89**, 59 (1994).
[52] G. Peris, J. Planelles, and J. Paldus, Int. J. Quantum Chem. **62**, 137 (1997).
[53] X. Li, G. Peris, J. Planelles, F. Rajadell, and J. Paldus, J. Chem. Phys. **107**, 90 (1997).
[54] G. Peris, F. Rajadell, X. Li, J. Planelles, and J. Paldus, Mol. Phys. **94**, 235 (1998).
[55] J. Planelles, G. Peris, and J. Paldus, Int. J. Quantum Chem. **77**, 693 (2000).
[56] X. Li and J. Paldus, J. Chem. Phys. **107**, 6257 (1997).
[57] J. Paldus and X. Li, in *Correlation and Localization, Topics in Current Chemistry*, edited by P. R. Surján (Springer, Berlin, 1999), Vol. 203, pp. 1–20.
[58] J. Paldus and X. Li, in *Advances in Quantum Many-Body Theory*, edited by R. F. Bishop, T. Brandes, K. A. Gernoth, N. R. Walet, and Y. Xian (World Scientific, Singapore, 2002), Vol. 5, pp. 393–404.
[59] X. Li and J. Paldus, in *Low-Lying Potential-Energy Surfaces*, ACS Symposium Series No. 828, edited by M. R. Hoffmann and K. G. Dyall (ACS, Washington, 2002), pp. 10–30.
[60] X. Li and J. Paldus, J. Chem. Phys. **108**, 637 (1998).
[61] X. Li and J. Paldus, J. Chem. Phys. **124**, 174101 (2006).
[62] X. Li and J. Paldus, J. Chem. Phys. **126**, 224304 (2007).
[63] X. Li and J. Paldus, Int. J. Quantum Chem. **108**, 2117 (2008).
[64] X. Li and J. Paldus, J. Chem. Phys. **129**, 174101 (2008).
[65] X. Li and J. Paldus, J. Theor. Comput. Chem. **7**, 805 (2008).
[66] X. Li and J. Paldus, Can. J. Chem. **87**, 917 (2009).
[67] D. W. Whitman and B. K. Carpenter, J. Am. Chem. Soc. **104**, 6473 (1982).
[68] B. K. Carpenter, J. Am. Chem. Soc. **105**, 1700 (1983).
[69] B. A. Hess, P. Čársky, and L. J. Schaad, J. Am. Chem. Soc. **105**, 695 (1983).
[70] A. F. Voter and W. A. Goddard III, J. Am. Chem. Soc. **108**, 2830 (1986).
[71] P. Čársky, R. J. Bartlett, G. Fitzgerald, J. Nova, and V. Špirko, J. Chem. Phys. **89**, 3008 (1988).
[72] B. R. Arnold and J. Michl, J. Phys. Chem. **97**, 13348 (1993).
[73] A. Balková and R. J. Bartlett, J. Chem. Phys. **101**, 8972 (1994).
[74] W. Wu, Y. Mo, Z. Cao, and Q. Zhang, Theor. Comput. Chem. **10**, 143 (2002).
[75] S. V. Levchenko and A. I. Krylov, J. Chem. Phys. **120**, 175 (2004).
[76] O. Demel and J. Pittner, J. Chem. Phys. **124**, 144112 (2006).
[77] S. Saddique and G. A. Worth, Chem. Phys. **329**, 99 (2006).
[78] M. Eckert-Maksić, M. Vazdar, M. Barbatti, H. Lischka, and Z. B. Maksić, J. Chem. Phys. **125**, 064310 (2006).
[79] O. Demel, K. R. Shamasundar, L. Kong, and M. Nooijen, J. Phys. Chem. A **112**, 11895 (2008).
[80] K. Bhaskaran-Nair, O. Demel, and J. Pittner, J. Chem. Phys. **129**, 184105 (2008).
[81] P. B. Karadakov, J. Phys. Chem. A **112**, 7303 (2008).
[82] K. Jankowski and J. Paldus, Int. J. Quantum Chem. **18**, 1243 (1980).
[83] X. Li and J. Paldus, J. Chem. Phys. **131**, 044121 (2009).
[84] X. Li and J. Paldus, Chem. Phys. Lett. **286**, 145 (1998).
[85] X. Li and J. Paldus, Collect. Czech. Chem. Commun. **63**, 1381 (1998).
[86] X. Li and J. Paldus, J. Chem. Phys. **110**, 2844 (1999).
[87] X. Li and J. Paldus, Mol. Phys. **98**, 1185 (2000).
[88] X. Li and J. Paldus, Int. J. Quantum Chem. **80**, 743 (2000).
[89] X. Li and J. Paldus, J. Chem. Phys. **113**, 9966 (2000).
[90] X. Li and J. Paldus, J. Chem. Phys. **118**, 2470 (2003).
[91] X. Li and J. Paldus, J. Chem. Phys. **125**, 164107 (2006).
[92] X. Li and J. Paldus, J. Phys. Chem. A **111**, 11189 (2007).
[93] X. Li and J. Paldus, J. Chem. Phys. **126**, 234303 (2007).
[94] X. Li and J. Paldus, Int. J. Quantum Chem. **109**, 3305 (2009).
[95] X. Li and J. Paldus, J. Chem. Phys. **119**, 5320 (2003).
[96] X. Li and J. Paldus, J. Chem. Phys. **119**, 5346 (2003).
[97] X. Li and J. Paldus, Int. J. Quantum Chem. **99**, 914 (2004).
[98] J. Paldus, X. Li, and N. D. K. Petraco, J. Math. Chem. **120**, 5890 (2004).
[99] X. Li and J. Paldus, J. Chem. Phys. **124**, 034112 (2006).
[100] T. H. Dunning, Jr., and P. J. Hay, in *Methods of Electronic Structure Theory*, edited by H. F. Shaefer III (Plenum, New York, 1977), Chap. 1, pp. 1–27.
[101] J. D. Watts, J. Gauss, and R. J. Bartlett, J. Chem. Phys. **98**, 8718 (1993).
[102] T. H. Dunning Jr., J. Chem. Phys. **90**, 1007 (1989).
[103] P. Piecuch, N. Oliphant, and L. Adamowicz, J. Chem. Phys. **99**, 1875 (1993).
[104] P. Piecuch and L. Adamowicz, J. Chem. Phys. **100**, 5792 (1994).
[105] NIST Chemistry Webbook, http://webbook.nist.gov/chemistry.
[106] M. W. Schmidt, K. K. Baldridge, J. A. Boatz, S. T. Elbert, M. S. Gordon, J. H. Jensen, S. Koseki, N. Matsunaga, K. A. Nguyen, S. J. Su, T. L. Windus, M. Dupuis, and J. A. Montgomery, J. Comput. Chem. **14**, 1347 (1993).
[107] See EPAPS supplementary material at http://dx.doi.org/10.1063/1.3225203 for the reference RHF, MCSCF, and FCI energies.
[108] X. Li and J. Paldus, J. Chem. Phys. **130**, 164116 (2009).